



**Universiteit
Leiden**
The Netherlands

Volume-weighted unipolar voltage predicts heart failure mortality in patients with dilated cardiomyopathy and ventricular arrhythmias

Kimura, Y.; Beukers, H.K.C.; Rademaker, R.; Chen, S.P.; Ebert, M.; Jensen, T.; ... ; Zeppenfeld, K.

Citation

Kimura, Y., Beukers, H. K. C., Rademaker, R., Chen, S. P., Ebert, M., Jensen, T., ... Zeppenfeld, K. (2023). Volume-weighted unipolar voltage predicts heart failure mortality in patients with dilated cardiomyopathy and ventricular arrhythmias. *Jacc: Clinical Electrophysiology*, 9(7), 965-975. doi:10.1016/j.jacep.2022.11.015

Version: Publisher's Version
License: [Creative Commons CC BY 4.0 license](https://creativecommons.org/licenses/by/4.0/)
Downloaded from: <https://hdl.handle.net/1887/3720817>

Note: To cite this publication please use the final published version (if applicable).

ORIGINAL RESEARCH

Volume-Weighted Unipolar Voltage Predicts Heart Failure Mortality in Patients With Dilated Cardiomyopathy and Ventricular Arrhythmias



Yoshitaka Kimura, MD, PhD,^{a,b} Hans K.C. Beukers, MD,^a Robert Rademaker, MD,^{a,b} H. Sophia Chen, MD,^{a,b} Micaela Ebert, MD,^{a,c} Thomas Jensen, MD,^{b,d} Sebastiaan R. Piers, MD, PhD,^{a,b} Adrianus P. Wijnmaalen, MD, PhD,^{a,b} Marta de Riva, MD, PhD,^{a,b} Olaf M. Dekkers, MD, PhD,^e William G. Stevenson, MD,^f Katja Zeppenfeld, MD, PhD^{a,b}

ABSTRACT

BACKGROUND Patients with dilated cardiomyopathy (DCM) who are undergoing catheter ablation of ventricular arrhythmias (VAs) are at risk of rapidly progressive heart failure (HF). Endocardial voltages decrease with loss of viable myocardium. Global left ventricular (LV) voltage as a surrogate for the amount of remaining viable myocardium may predict prognosis.

OBJECTIVES This study evaluated whether the newly proposed parameter volume-weighted (vw) unipolar voltage (UV) can predict HF-related adverse outcomes (HFOs), including death, heart transplantation, or ventricular assist device implantation, in DCM.

METHODS In consecutive patients with DCM referred for VA ablation, vwUV was calculated by mathematically integrating UV over the left ventricle, divided by the endocardial LV surface area and wall thickness. Patients were followed for HFOs.

RESULTS A total of 103 patients (57 ± 14 years of age; left ventricular ejection fraction [LVEF], 39% ± 13%) were included. Median vwUV was 9.75 (IQR: 7.27-12.29). During a median follow-up of 24 months (IQR: 8-47 months), 25 patients (24%) died, and 16 had HFOs 7 months (IQR: 1-18 months) after ablation. Patients with HFOs had significantly lower LVEF (29% ± 10% vs 41% ± 12%), vw bipolar voltage (BV) (3.00 [IQR: 2.47-3.53] vs 5.00 [IQR: 4.12-5.73]), and vwUV (5.94 [IQR: 5.28-6.55] vs 10.37 [IQR: 8.82-12.81]; all $P < 0.001$), than patients without HFOs. In Cox regression analysis and goodness-of-fit tests, vwUV was the strongest and independent predictor for HFOs (HR: 3.68; CI: 2.09-6.45; likelihood ratio chi-square, 33.05; $P < 0.001$).

CONCLUSIONS The novel parameter vwUV, as a surrogate for the amount of viable myocardium, identifies patients with DCM with VA who are at high risk for HF progression and mortality. (J Am Coll Cardiol EP 2023;9:965-975)

© 2023 by the American College of Cardiology Foundation.

From the ^aDepartment of Cardiology, Heart-Lung Center, Leiden University Medical Center, Leiden, the Netherlands; ^bWillem Einthoven Center of Arrhythmia Research and Management, Leiden University Medical Center, Leiden, the Netherlands; ^cHeart Center Dresden, Department of Cardiology, Technical University Dresden, Dresden, Germany; ^dDepartment of Cardiology, Aarhus University Hospital, Aarhus, Denmark; ^eDepartment of Clinical Epidemiology, Leiden University Medical Center, Leiden, the Netherlands; and the ^fDepartment of Cardiology, Vanderbilt University Medical Center, Nashville, Tennessee, USA. The authors attest they are in compliance with human studies committees and animal welfare regulations of the authors' institutions and Food and Drug Administration guidelines, including patient consent where appropriate. For more information, visit the [Author Center](#).

Manuscript received June 3, 2022; revised manuscript received November 8, 2022, accepted November 20, 2022.

ABBREVIATIONS AND ACRONYMS

AWT	= average wall thickness
BV	= bipolar voltage
CMR	= cardiac magnetic resonance
CT	= computed tomography
DCM	= dilated cardiomyopathy
EAM	= electroanatomical mapping
EAVM	= electroanatomical voltage mapping
ECV	= extracellular volume
HF	= heart failure
HFmrEF	= heart failure with mildly reduced ejection fraction
HFO	= heart failure-related adverse outcome
HFpEF	= heart failure with preserved ejection fraction
HFREF	= heart failure with reduced ejection fraction
HNDPCM	= hypokinetic nondilated cardiomyopathy
HT	= heart transplantation
LGE	= late gadolinium enhancement
LR	= likelihood ratio
LV	= left ventricular
LVA	= low voltage area
LVAD	= left ventricular assist device
LVEF	= left ventricular ejection fraction
NT-proBNP	= N-terminal pro-B-type natriuretic peptide
PVC	= premature ventricular contraction
RFCA	= radiofrequency catheter ablation
ROC	= receiver-operating characteristic
UV	= unipolar voltage
VA	= ventricular arrhythmia
VT	= ventricular tachycardia
vwBV	= volume-weighted bipolar voltage
vwUV	= volume-weighted unipolar voltage
WT	= wall thickness

Patients with nonischemic dilated cardiomyopathy (DCM) and ventricular arrhythmias (VAs) are at high risk of heart failure (HF)-related death.¹ Diffuse fibrosis plays an important role in the development of HF. Cardiac magnetic resonance (CMR) has been proposed to delineate regional and diffuse fibrosis noninvasively. Of note, an increase in extracellular volume (ECV) fraction, which reflects diffuse myocardial fibrosis,^{2,3} may precede impairment of left ventricular (LV) systolic function.² The extent of ECV fraction increase provides prognostic information on HF outcome in addition to late gadolinium enhancement (LGE), which visualizes regional scar.^{4,5}

Unipolar electroanatomical voltage mapping (EAVM), routinely performed in patients undergoing VA ablation, correlates with fibrosis and can detect fibrosis not evident on CMR in patients with DCM.⁶ Unipolar voltage (UV) cutoff values for normal human left ventricles have been derived from young, healthy control subjects.⁷ Of importance, from analysis of EAVM and histologic fibrosis in explanted human hearts with DCM, we found linear relationships between UV and the amount of transmural viable myocardium and between UV and wall thickness (WT).^{6,8}

On the basis of these data, we propose a new parameter, volume-weighted (vw) UV, as a surrogate for the total amount of remaining viable myocardium. We hypothesized that a critical reduction in vwUV may identify patients at risk to develop rapid deterioration of cardiac function and end-stage HF.

METHODS

PATIENT GROUP. Consecutive patients with DCM or hypokinetic nondilated cardiomyopathy (HNDPCM)⁹ who were referred for radiofrequency catheter ablation (RFCA) of VA to the Leiden University Medical Center (Leiden, the Netherlands) between June 2011 and March 2018 were enrolled. Patients with significant coronary artery disease, defined by >75% coronary artery stenosis, congenital

heart disease, hypertrophic cardiomyopathy, restrictive cardiomyopathy, biopsy-proven myocarditis, cardiac sarcoidosis, LV noncompaction, or primary valvular disease were excluded. The study was

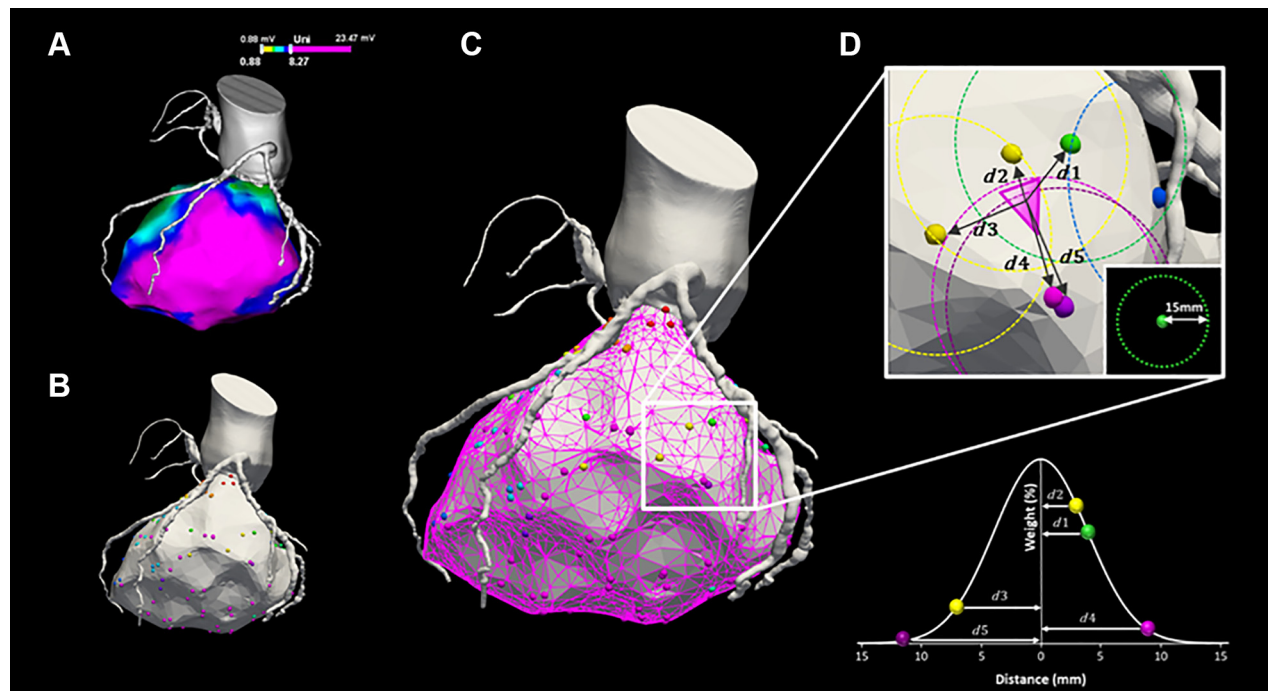
approved by the Dutch local ethical committee (G21.120).

PREPROCEDURAL ANALYSIS. All patients underwent a comprehensive clinical evaluation. Echocardiographic measurements of the left ventricle, including WT (intraventricular septum and posterior wall) were performed in the parasternal long-axis view.¹⁰ LV WT was also measured by contrast computed tomography (CT) in 20 patients where preprocedural contrast CT was available and was compared with echocardiography-derived WT. Using MASS Research Software (Research version 2018, LKEB, Leiden University Medical Center), endocardial and epicardial LV contours were manually drawn on the short-axis CT images, and the average WT (AWT) was automatically calculated.

LV ejection fraction (LVEF) was assessed with the biplane Simpson method.¹⁰ On the basis of the 2021 European Society of Cardiology guidelines for the diagnosis and treatment of HF, HF with preserved ejection fraction (HFpEF), HF with mildly reduced EF (HFmrEF), and HF with reduced EF (HFREF) were defined by LVEF $\geq 50\%$, 41% to 49%, and $\leq 40\%$, respectively.¹¹ Kidney disease was defined as an estimated glomerular filtration rate of < 45 mL/min/1.73 m² (chronic kidney disease stage ≥ 3 B). Genetic testing by combined next-generation and Sanger sequencing of ≥ 55 cardiomyopathy-related genes was performed as previously described.¹² All antiarrhythmic agents (except for amiodarone) were discontinued before mapping and ablation.

ELECTROANATOMICAL MAPPING AND ABLATION. The procedure was performed with the patient under conscious sedation, deep sedation, or general anesthesia, when indicated. All patients underwent endocardial electroanatomical mapping (EAM) of the aortic root and left ventricle during baseline rhythm by using the CARTO3 system (Biosense Webster, Inc). Mapping was performed using a 3.5-mm electrode tip catheter (NaviStar ThermoCool or Thermocool Smarttouch, Biosense Webster) with a fill threshold of ≤ 10 millimeters. Catheter tip-to-tissue contact was confirmed by stable electrogram recordings and/or contact force. In almost all cases, retrograde and transseptal access was obtained to facilitate catheter contact. All EAM was performed by an experienced operator. Electrograms were filtered at 30 to 400 Hz (bipolar) and 1 to 240 Hz (unipolar) and were displayed at 200 mm/s sweep speed. Confluent areas of endocardial low bipolar voltage (BV) (< 1.5 mV) and UV (< 8.27 mV) were defined as low-voltage areas (LVA).¹³ The positions of the aortic and mitral valve

FIGURE 1 Electroanatomical Mapping Data Processing and Interpolation Method



(A) The electroanatomical mapping was reviewed to remove the valve areas and the mapping points with premature ventricular contractions or artifacts and to adapt the mapping window of interest. (B) The corrected mapping points and (C) 3-dimensional mesh files obtained from the CARTO system (Biosense Webster, Inc.) were transferred and visualized in ParaView (Kitware, Inc.). (D, top) The bipolar voltage and unipolar voltage values for each triangle of the 3-dimensional mesh were calculated by interpolating the voltages of the surrounding measured electroanatomical mapping contact points. (D, bottom) A maximum inclusion radius from the electroanatomical mapping point and a Gaussian distribution were used for interpolation, as described in the text.

annuli were determined on the basis of the aortic root map and local electrograms. All mapping and ablation procedures were continuously recorded for off-line analysis. The details of the induction protocol, the ablation procedure, and the definition of procedural outcomes are described in [Supplemental Method 1](#).

LONG-TERM OUTCOME. Patients were routinely followed at the outpatient clinic 3, 6, and 12 months after RFCA and every 6 to 12 months afterward. Follow-up included medical history, implantable cardioverter-defibrillator interrogation, and repeat echocardiography ≥ 3 months after ablation and on clinical indication thereafter.

The primary endpoint was an HF-related adverse outcome (HFO), defined as HF death, heart transplantation (HT), or left ventricular assist device (LVAD) implantation. Causes of death were categorized into sudden cardiac death, HF death, other cardiovascular deaths, or noncardiac death.

The secondary endpoint was LVEF deterioration, defined as a $>5\%$ decrease of LVEF from baseline and transition to a worse HF category (from HFpEF to

HFmrEF or from HFmrEF to HFrEF). For the analysis, the latest available echocardiography was evaluated. If LVEF deterioration was noted, the first time when LVEF deterioration occurred was determined by reviewing all previous echocardiography reports. A detailed definition of all endpoints and the follow-up is provided in [Supplemental Method 2](#).

ELECTROANATOMICAL MAPPING ANALYSIS. QRS complex duration at baseline was measured with electronic calipers. All electrograms were reviewed off-line by an independent examiner on the CARTO system to confirm the stability of the electrogram by comparing it with the previous beats. Premature ventricular contractions (PVCs) were removed. For each point, the mapping window of interest was manually adapted to exclude far-field electrograms, artifacts, and electrogram changes resulting from injury current from the peak-to-peak measurement of BV and UV amplitudes. LVAs, the total LV endocardial surface area, and the LV volume were assessed using the CARTO area and volume measurement tools, after excluding the aortic and mitral valve areas. The total

percentage of LVA was calculated by dividing the LVA by the total LV endocardial surface area.

AREA AND VOLUME-WEIGHTED BIPOLAR AND UNIPOLAR VOLTAGES. After manual correction and removal of the aortic and mitral valve areas, the endocardial EAM data and 3-dimensional meshes were transferred from CARTO to ParaView 3-dimensional visualization software version 5.7 (Kitware, Inc) by using custom-made Python plugins (Figures 1A to 1C). To calculate area and volume-weighted bipolar and unipolar voltages (vwBV, vwUV) the following mathematical steps were performed (Figure 1D).

1. The BV and UV values at each location on the LV endocardial surface mesh were determined by interpolating the voltages of the surrounding measured EAM contact points. The interpolation corrects for differences of local mapping density and distances between points. The interpolation uses the weighted average of the EAM points within a specified radius and a Gaussian distribution to assign the weights. This interpolation ensures that adjacent points contribute more to the interpolated voltages than distant points. The weighting function for the Gaussian interpolation method is the Gaussian distribution:

$$w(d, \sigma) = a \exp(1/2 [d/\sigma]^2)$$

where d is the distance from an EAM point to interpolated point, σ is the width of the distribution, and a is a normalization factor, ensuring that the sum of all weights is 1 (Supplemental Method 3).

2. The integrated BV and UV were calculated by mathematically integrating the BV and UV over the LV surface. For this step, the interpolated value of each triangle of the mesh was multiplied by its surface area, and the results for all triangles were summed together. The area-weighted BV and UV (awBV and awUV) were determined by dividing the integrated BV and UV by the total LV endocardial surface area.
3. The vwBV and vwUV were acquired by dividing the awBV and awUV by the AWT of the intraventricular septum and posterior wall on the basis of the assumption that BV and UV have a linear relationship with the corresponding WT.⁶

STATISTICAL ANALYSIS. Categorical variables are displayed as numbers (percentages) and continuous variables as mean \pm SD when normally distributed or median with IQR when not normally distributed. Categorical variables were compared using the chi-square or Fisher exact test. Continuous variables were compared with Student's t -test. Receiver-

operating characteristic (ROC) curve analysis was performed to determine the optimal cutoff value for vwUV to predict HFO, defined as the values maximizing the sum of sensitivity and specificity. Survival curves were estimated by the Kaplan-Meier method and were compared by the log-rank test. Univariable Cox proportional hazard analysis was used to test the association between HFO (freedom from HFO) and baseline covariables. Independent predictors of HFO were analyzed with 3 different multivariable models: 1) age, significant baseline clinical variables in univariable analysis, and vwUV were included; 2) all variables significant in univariable analysis were included; and 3) a backward stepwise selection was used. Variables with $P < 0.10$ were initially included. At each step, the least significant variable was removed from the model until all variables reached $P < 0.20$. All tests were 2-sided, and a P value < 0.05 was considered statistically significant.

To evaluate the additional value of mapping-derived parameters to identify patients at risk of HFO, models containing a propensity base score were created and compared with models consisting of the propensity score in addition to the additional parameter. The models were compared using a goodness-of-fit test. Propensity scores were calculated using Cox regression to correct for potential clinical confounders and simplifying the calculations for the likelihood ratios (LRs). Age, sex, and all clinical variables associated with HFO in the univariable Cox regression analysis (kidney disease, N-terminal pro-B-type natriuretic peptide [NT-proBNP], [likely] pathogenic genetic mutation, LVEF, and amiodarone use at baseline) were included. Using these propensity scores, all LR calculations were performed on models created by the following steps. First, the base propensity score for the outcome was calculated. Then, each of the following variables was added in a separate model: bipolar and unipolar LVAs; vwBV; and vwUV. For each of these models containing 2 variables (propensity score and the variable to be tested), the LR in comparison with the base model (containing just the propensity score) was calculated. The increased LR was significant if the LR chi-square test showed a P value < 0.05 . If that was the case, the added variable was deemed an improvement over the base model. All analyses were performed using SPSS software version 25.0 (IBM Corp).

RESULTS

BASELINE, ELECTROANATOMICAL MAPPING, AND ABLATION DATA. A total of 103 patients with DCM or HNDCM (57 ± 14 years of age; 81% men) who were

referred for catheter ablation of VAs (sustained monomorphic VT, n = 83 [81%]; PVC, n = 20 [19%]) were enrolled. The mean LVEF was 39% ± 13%, and the median NT-proBNP value was 773 pg/mL (IQR: 254-4,646 pg/mL). Genetic testing was performed in all but 2 patients, with a (likely) pathogenic mutation in 33 patients (32%). Baseline characteristics are summarized in **Table 1**.

LV EAVM was performed in nonpaced rhythm (n = 82) or during right ventricular pacing (n = 21) before RFCA. In the 83 patients referred for VT ablation, a median of 3 sustained monomorphic VTs (IQR: 1-5) could be induced. RFCA was performed in 78 patients (epicardial in 44). The median ablation time was 11 minutes (IQR: 6-20 minutes). In 5 patients, no ablation was performed because of the absence of accessible target sites. Complete procedural success was achieved in 34 (44%), partial success was achieved in 42 (54%), and the procedure failed in 2 cases (3%). Two patients had cardiac tamponade, which was controlled by pericardial drainage. No significant HF worsening after ablation was observed. Of the 20 patients who were referred for PVC ablation, 16 underwent RFCA with procedural success in 69%. In 4 patients, no ablation was performed because of infrequent PVCs.

FOLLOW-UP. During a median follow-up of 24 months (IQR: 8-47 months), 22 patients (21%) died (13 HF, 3 sudden cardiac death, 6 noncardiac death), and in 16 (16%) an HFO occurred (HF death, 13; HT or LVAD, 3) after a median time from ablation of 7 months (IQR: 1-18 months). No HFOs were caused by uncontrollable VT. VT recurred in 47 (46%) patients. Kaplan-Meier estimates of all-cause mortality, HT, or LVAD and HFO at 1 year and 2 years after RFCA were 13% and 24% (for all-cause mortality, HT, or LVAD) and 9% and 16% (for HFO), respectively. The modes of deaths are summarized in **Supplemental Table 1**.

BASILINE, ELECTROANATOMICAL MAPPING, AND ABLATION DATA ACCORDING TO HFO. Patients with HFO more frequently had kidney disease, a pathogenic or likely pathogenic mutation, and a worse LVEF at baseline evaluation, compared with patients without HFO (**Table 1**). In terms of EAM-derived data, patients with HFO had a larger mean LV surface area, LV volume, and bipolar and unipolar LVAs than those without an event. Furthermore, vwBV and vwUV were significantly decreased in patients with HFO (vwBV 3.00 [IQR: 2.47-3.53] vs 5.00 [IQR: 4.12-5.73]; vwUV 5.61 [IQR: 4.86-6.25] vs 10.19 [IQR: 8.76-12.77]; both *P* < 0.001) (**Table 2, Figure 2**). ROC curve analysis showed that vwUV had a high diagnostic accuracy for consecutive HFO (cutoff 6.59; area under the curve

TABLE 1 Baseline Characteristics

	Overall (N = 103)	HFO (-) (n = 87)	HFO (+) (n = 16)	P Value
Age, y	57 ± 14	57 ± 14	60 ± 14	0.38
Male	83 (81)	70 (80)	13 (81)	1.0
Hypertension	37 (36)	31 (36)	6 (38)	1.0
Diabetes mellitus	16 (16)	13 (15)	3 (19)	0.71
Kidney disease	10 (10)	6 (7)	4 (25)	0.047
History of AF	29 (28)	24 (28)	5 (31)	0.77
NT-proBNP, pg/mL	773 (254-1,646)	642 (212-1,291)	2,576 (1,397-4,670)	<0.001
(Likely) pathogenic genetic variant	33 (32)	23 (26)	10 (63)	0.008
QRS width, ms	108 (95-153)	107 (93-153)	138 (99-157)	0.28
LVEF, %	39 ± 13	41 ± 12	29 ± 10	<0.001
LVDD, cm	60 ± 8	59 ± 9	64 ± 8	0.07
AWT, cm	0.95 ± 0.15	0.94 ± 0.13	0.99 ± 0.17	0.20
IVSD, cm	0.97 ± 0.18	0.96 ± 0.16	1.00 ± 0.17	0.34
LVPWD, cm	0.94 ± 0.15	0.93 ± 0.14	0.98 ± 0.21	0.18
ACE inhibitor or ARB	79 (77)	68 (78)	11 (69)	0.52
MRA	33 (32)	26 (30)	7 (44)	0.38
β-Blocker	70 (68)	59 (68)	11 (69)	1.0
Amiodarone	36 (35)	25 (29)	11 (69)	0.004
ICD present before ablation	69 (67)	53 (61)	16 (100)	0.001
CRT present before ablation	31 (30)	24 (28)	7 (44)	0.24

Values are mean ± SD, n (%), or median (IQR).
 ACE = angiotensin-converting enzyme; AF = atrial fibrillation; ARB = angiotensin II receptor blocker; AWT = average wall thickness; CRT = cardiac resynchronization therapy; ICD = intracardiac cardioverter-defibrillator; HFO = heart failure-related adverse outcome; IVSD = intraventricular septum dimension; LVDD = left ventricular diastolic dimension; LVEF = left ventricular ejection fraction; LVPWD = left ventricular posterior wall dimension; MRA = mineralocorticoid receptor antagonist; NT-proBNP = N-terminal pro-B-type natriuretic peptide; (+) = present; (-) = absent.

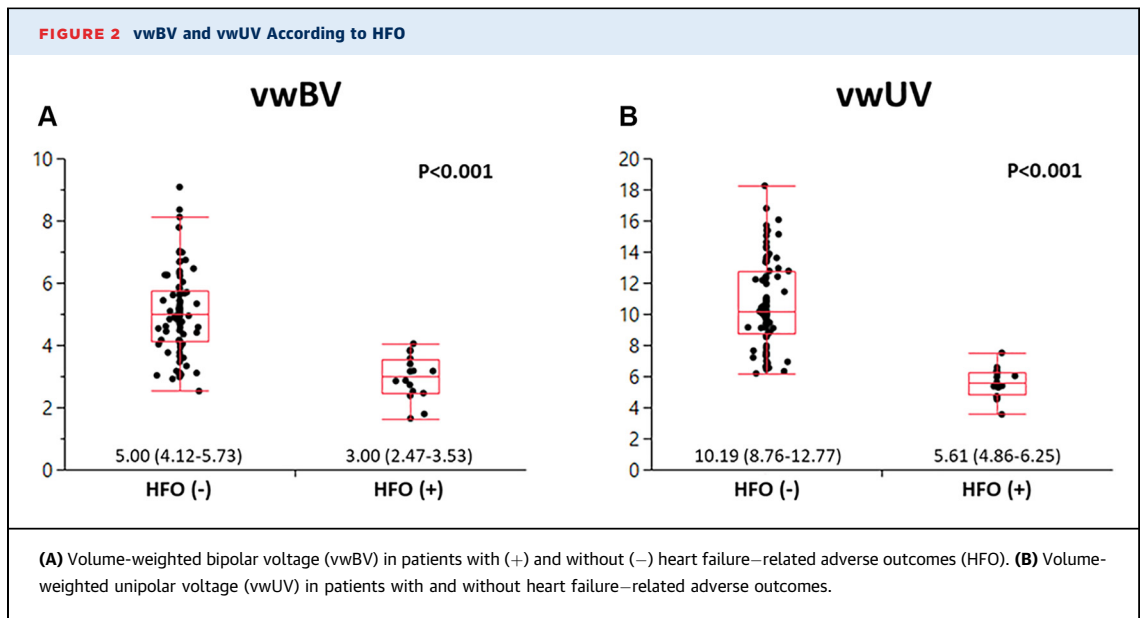
[AUC], 0.98; sensitivity, 94%; specificity, 95%) (**Supplemental Figure 1A**). A strong correlation between echocardiography- and CT-derived AWTs was observed (**Supplemental Figure 2**).

PREDICTION OF OUTCOME. In univariable Cox regression analysis, log NT-proBNP, LVEF, amiodarone use, vwUV, vwBV, bipolar and unipolar LVAs, and short-term acute procedural outcome were

TABLE 2 Electroanatomical Mapping-Derived Data

	Overall (N = 103)	HFO (-) (n = 87)	HFO (+) (n = 16)	P Value
Surface, cm ²	180 ± 49	173 ± 48	216 ± 38	0.001
LV volume, cm ³	208 ± 92	198 ± 91	262 ± 81	0.001
Bipolar LVA, cm ²	4 (1-17)	2 (1-10)	24 (8-64)	<0.001
Unipolar LVA, cm ²	73 (31-118)	55 (22-96)	162 (125-215)	<0.001
Bipolar LVA, %	2 (1-10)	2 (0-5)	12 (5-30)	<0.001
Unipolar LVA, %	35 (17-55)	27 (13-48)	74 (59-92)	<0.001
Integrated BV	753 (604-789)	804 (625-987)	572 (485-670)	<0.001
vwBV	4.83 (3.59-5.60)	5.00 (4.12-5.73)	3.00 (2.47-3.53)	<0.001
Integrated UV	1,567 (1,195-1,946)	1,659 (1,375-2,061)	1,105 (984-1,331)	<0.001
vwUV	9.75 (7.27-12.29)	10.19 (8.76-12.77)	5.61 (4.86-6.25)	<0.001

Values are mean ± SD or median (IQR).
 BV = bipolar voltage; LV = left ventricular; LVA = low-voltage area; UV = unipolar voltage; vwBV = volume-weighted bipolar voltage; vwUV = volume-weighted unipolar voltage; other abbreviations as in **Table 1**.



significantly associated with HFO (Table 3). In all 3 models of multivariable Cox regression analyses, only vwUV remained significantly associated with HFO (Table 3).

GOODNESS-OF-FIT TESTS. After adjustment for parameters that influence the risk for HFO in a propensity score, vwUV most significantly increased the LR for HFO (LR chi-square, 33.05; $P < 0.001$) (Table 4), followed by awUV (23.22) and unipolar LVA (18.82).

ELECTROANATOMICAL MAPPING-DERIVED DATA ACCORDING TO HF CATEGORIES. The proportions of HFpEF, HFmrEF, and HFrfEF were 21%, 27%, and 51% of the patients, respectively (Supplemental Table 2). LV surface area and LV volume increased with decreasing LVEF (LV surface area, $R^2 = 0.28$; LV volume, $R^2 = 0.24$; $P < 0.001$ for both) (Supplemental Figure 3), with statistically significant differences between HFpEF and HFmrEF ($P < 0.001$) (Supplemental Table 3). Bipolar and unipolar LVAs (absolute and as a percentage of LV surface) were significantly smaller in HFpEF compared with HFmrEF, but they showed no significant difference between patients with HFmrEF and HFrfEF. Of note, integrated BV and UV were not significantly different across the 3 groups (Supplemental Table 3). However, after correcting for the LV wall volume, vwBV and, in particular, vwUV were significantly larger in patients with HFpEF compared with patients with HFmrEF, but they were similar between patients with HFmrEF and those with HFrfEF (Central Illustration).

OUTCOME ACCORDING TO HF CATEGORIES. Among patients with HFmrEF and HFrfEF, 5 (18%) and 11 (21%) patients had HFO, respectively, whereas all patients with HFpEF survived without the need for HT or LVAD placement. ROC curve analyses showed that AUCs of vwUV for HFO were 0.94 (cutoff, 7.50; sensitivity, 100%; specificity, 82%) and 0.99 (cutoff, 6.57; sensitivity, 100%; specificity, 93%) in patients with HFmrEF and HFrfEF, respectively (Supplemental Figures 1B and 1C). When patients with HFmrEF and with HFrfEF were stratified according to the medians of vwUV, Kaplan-Meier analysis showed an excellent prognosis for those with vwUV >7.50 and >6.57 , respectively (log-rank $P < 0.001$ in both) (Figures 3B and 3C).

In 80 patients (78%), echocardiographic follow-up data obtained after a median duration from the EAM to the latest echocardiography of 32 months (IQR: 11-58 months) were available. Among HFpEF and HFmrEF patients, LVEF deterioration occurred in 2 of 18 (11%) and in 6 of 24 (25%) patients, respectively. Importantly, among patients with HFmrEF and disease progression, LVEF deterioration occurred within the first year after EAM in 5 of 6 (83%) with progression to HFO in 4 of 5 (80%) patients. In the 2 patients with HFpEF and LVEF deterioration, LVEF deterioration was observed 22 and 34 months after EAM.

Of interest, patients with HFmrEF and vwUV >7.50 also had a favorable prognosis regarding future LVEF deterioration (Figure 3A). Two representative cases in patients with HFmrEF are displayed in the Central Illustration. The clinical course of all 27 patients

TABLE 3 Univariable and Multivariable Analyses for Heart Failure-Related Adverse Outcomes

	Univariable Analysis			Multivariable Analysis								
	HR	95% CI	P Value	Model 1			Model 2			Model 3		
				HR	95% CI	P Value	HR	95% CI	P Value	HR	95% CI	P Value
Age	1.03	0.99-1.07	0.22	0.96	0.91-1.03	0.22	—	—	—	—	—	—
Male	0.99	0.21-3.47	0.98	—	—	—	—	—	—	—	—	—
Kidney disease	3.50	1.12-11.01	0.03	3.35	0.45-27.4	0.23	4.39	0.28-63.8	0.28	—	—	—
AF	1.23	0.43-3.56	0.67	—	—	—	—	—	—	—	—	—
Log NT-proBNP	2.65	1.67-4.23	<0.001	1.21	0.58-2.44	0.59	1.00	0.50-2.08	0.99	—	—	—
(Likely) pathogenic genetic Variant	3.87	1.40-10.67	0.01	0.18	0.02-1.29	0.09	0.46	0.05-3.35	0.46	—	—	—
QRS width, 1-ms increase	1.01	0.99-1.02	0.16	—	—	—	—	—	—	—	—	—
LVEF, 1% decrease	1.10	1.05-1.17	<0.001	0.99	0.92-1.06	0.74	0.98	0.89-1.08	0.68	—	—	—
Amiodarone	5.14	1.76-14.99	0.003	2.77	0.51-17.3	0.24	1.56	0.20-11.2	0.66	—	—	—
vwBV, 1 decrease	4.59	2.59-8.13	<0.001	—	—	—	0.74	0.09-8.70	0.80	—	—	—
vwUV, 1 decrease	3.10	2.04-4.69	<0.001	4.14	2.13-40.0	<0.001	3.55	1.10-15.6	0.03	3.68	2.09-6.45	<0.001
Bipolar LVA, 1% increase	1.07	1.04-1.11	<0.001	—	—	—	1.03	0.95-1.12	0.51	—	—	—
Unipolar LVA, 1% increase	1.08	1.05-1.12	<0.001	—	—	—	1.02	0.96-1.09	0.54	—	—	—
Complete procedural success	4.44	1.23-16.1	0.02	—	—	—	3.03	0.45-34.2	0.27	—	—	—

Model 1: Age + significant baseline variables (kidney disease, log-proBNP, (likely) pathogenic genetic variant, LVEF, and amiodarone) + vowel; Model 2: All variables significant in univariable analysis; Model 3: Backward stepwise selection.
 Abbreviations as in Tables 1 and 2.

with HFmrEF is summarized in Supplemental Figure 4.

DISCUSSION

This is the first study to evaluate the performance of a novel parameter, vwUV, to predict HF-related adverse events in patients with DCM referred for ablation of VA. The main findings can be summarized as follows: 1) reduced vwUV available from routine voltage mapping was a strong predictor and the only independent predictor of HFO in patients with DCM; 2) vwUV had the highest incremental value for predicting HFO after adjustment for clinical factors known to be associated with HFO, including LVEF, NT-proBNP, and kidney disease; and 3) vwUV was strongly related to subsequent LVEF deterioration and HFO in patients with DCM with HFmrEF at the time of mapping.

The results suggest that a critical reduction of vwUV, as a surrogate for the total remaining viable myocardium at the time of evaluation, provides incremental prognostic information and may identify patients with DCM at risk for rapid progressive HF.

MORTALITY IN DILATED CARDIOMYOPATHY WITH VENTRICULAR ARRHYTHMIAS. In patients with DCM and VA who are referred for catheter ablation, subsequent mortality is high.^{12,14} Most deceased patients with DCM died of progressive HF.¹⁵ The high 1- and 2-year mortality rates after RFCA of 13% and 24%, respectively, in our cohort are in line with these data.

Similar to earlier studies, 16% of our patients had an adverse outcome because of end-stage HF, which was the dominant cause of death.

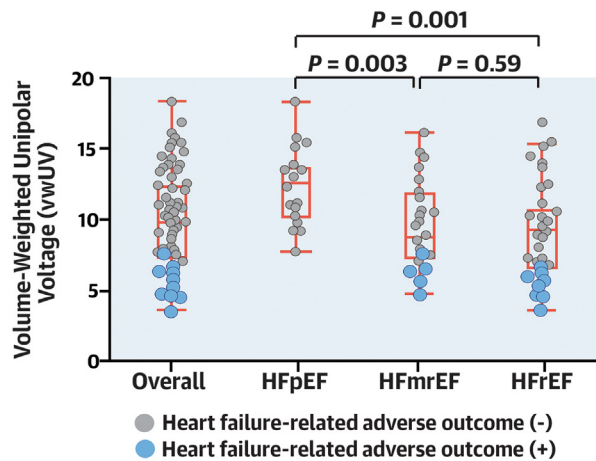
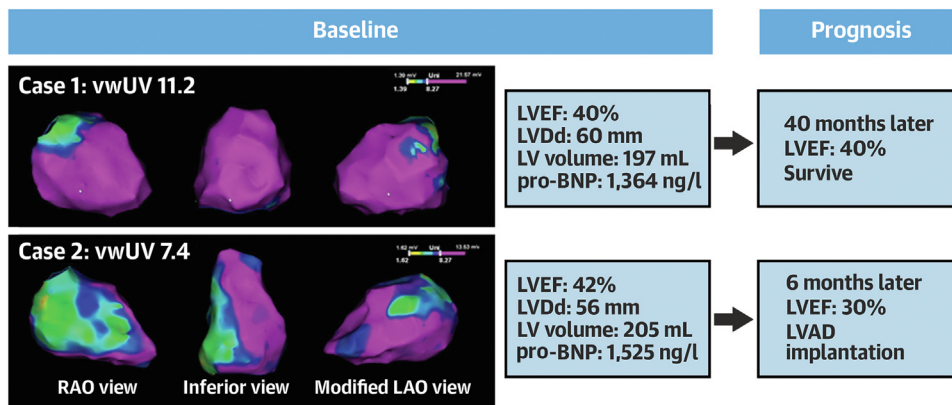
ROLE OF DIFFUSE MYOCARDIAL FIBROSIS IN DILATED CARDIOMYOPATHY.

Myocardial fibrosis is perhaps the most important structural abnormality in patients with DCM with VA.⁶ LGE detects areas of sizable replacement fibrosis but is less sensitive to interstitial fibrosis. Histologic analysis has shown a strong positive correlation between biopsy-proven collagen volume and the ECV fraction, as determined by CMR T₁ mapping.^{2,3} Significantly increased ECV has been recognized in “early DCM” patients with an LVEF of 45% to 55%, a finding suggesting that increased ECV may precede LVEF deterioration.² Of importance, native T₁ and ECV fraction outperform the presence of LGE, which visualizes regional scar, in predicting HFO and mortality in DCM.^{2,4,5}

TABLE 4 Goodness-of-Fit Test for Heart Failure-Related Adverse Outcomes

	LR Chi-Square	P Value
Base propensity score	N/A	N/A
+Bipolar LVA	3.45	0.06
+Unipolar LVA	18.82	<0.001
+awBV	8.66	0.003
+awUV	23.22	<0.001
+vwBV	15.63	<0.001
+vwUV	33.05	<0.001

awBV = area-weighted bipolar voltage; awUV = area-weighted unipolar voltage; LR = likelihood ratio; other abbreviations as in Tables 1 and 2.

CENTRAL ILLUSTRATION Distribution of Volume-Weighted Unipolar Voltage and Prognosis**A** Distribution of vwUV According to HF Category**B** Impact of vwUV on Prognosis in HFmrEF

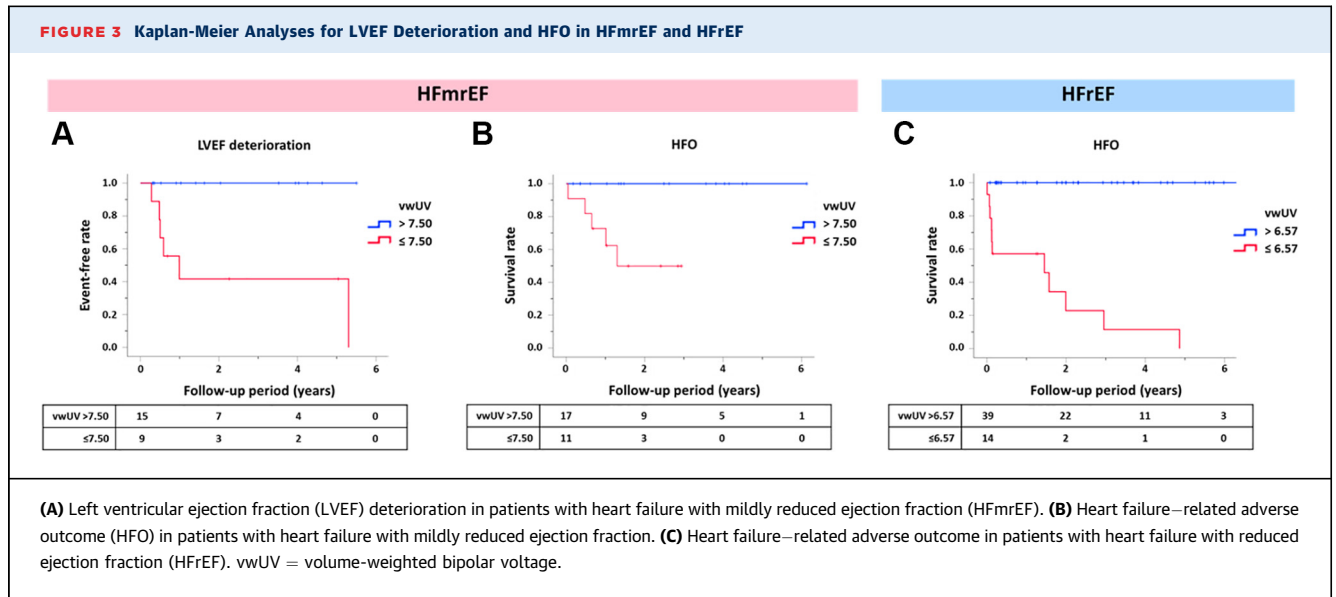
Kimura Y, et al. *J Am Coll Cardiol EP*. 2023;9(7):965-975.

(A) Distribution of volume-weighted unipolar voltage (vwUV) according to heart failure category. (B) Prognosis in 2 representative cases in patients with heart failure with mildly reduced ejection fraction (HFmrEF). HFO = heart failure-related adverse outcome; HFpEF = heart failure with preserved ejection fraction; HFrEF = heart failure with reduced ejection fraction; LAO = left anterior oblique; LV = left ventricular; LVAD = left ventricular assist device; LVd = left ventricular diastolic dimension; LVEF = left ventricular ejection fraction; pro-BNP = pro-B-type natriuretic peptide; RAO = right anterior oblique; (+) = present; (-) = absent.

ELECTROANATOMICAL MAPPING AS A SURROGATE FOR DISEASE SEVERITY. EAVM, which is routinely performed in patients undergoing VA ablation, is considered the invasive gold standard to detect fibrosis in DCM. Both UV and BV have a proportional relationship with the amount of biopsy-proven viable myocardium in DCM.⁶ However, BV largely reflects

subendocardial fibrosis, and UV is considered superior to BV in detecting midwall or subepicardial fibrosis in DCM with preserved WT because of its wider “field of view.”

Campos et al¹³ reported that a large (>33% of the endocardial surface) area with low UV defined as $UV < 8.27$ mV could distinguish between reversible



and irreversible LV dysfunction. Using the same voltage threshold, a unipolar LVA $>145 \text{ cm}^2$ (or $>70\%$ of the LV surface) was associated with cardiac mortality in a mixed cohort of 55 patients with non-ischemic cardiomyopathy and VT. Of note, in that study, the 11 patients with an event had already a very poor LVEF ($22\% \pm 6\%$) at baseline.¹⁶

In line with and further extending the findings of that report, unipolar LVA was a predictor of HFO in univariable analysis. However, after adjustment for clinical parameters, the newly proposed vwUV remained the only independent predictor of HFO in Cox regression multivariable analysis. The goodness-of-fit test further supported the incremental and superior prognostic value of vwUV compared with unipolar LVA.

LOW-VOLTAGE AREA VS VOLUME-WEIGHTED VOLTAGES. Determination of LVA requires a voltage threshold, and the exact size of the LVA depends on mapping density and the interpolation of voltages provided by the mapping system. Previous studies have applied UV $<8.27 \text{ mV}$, on the basis of the 5th percentile of UV in 6 subjects with structurally normal heart,⁷ to estimate the endocardial area with abnormal UV.^{13,16} On the basis of the comparison of LGE CMR and voltage mapping, a wide range (5.64–9.84 mV) of UV cutoffs has been proposed to detect regional nonischemic scar.^{17–19} Different LGE CMR acquisition protocols, postprocessing methods, and signal intensity thresholds have been used, and to date, there is no consensus on the most robust and reproducible approach. Considering the observed linear relationships between voltages and the amount

of viable myocardium and between voltages and WT in patients with DCM,⁶ any binary voltage threshold cannot reflect the extent and severity of the diseased myocardium.

To overcome these limitations, we developed and tested a novel parameter, vwUV. Weighted and interpolated voltages on the LV endocardial mesh are obtained using a Gaussian distribution, correcting for unevenly distributed mapping points. The awBV and awUV, which were obtained by correcting for LV surface area, were superior to bipolar and unipolar LVAs, respectively. We further corrected for WT, resulting vwUV, which provides an estimate for the viable mass per cubic centimeter. The superior and incremental prognostic value for HFO suggests that vwUV more accurately reflects the total amount of remaining viable myocardium in an individual patient.

VwUV AND LVEF DETERIORATION IN PATIENTS WITH HFmrEF. Efforts have been made to characterize HFmrEF patients more accurately.¹¹ Progression from HFmrEF to HFrEF is associated with a poor outcome.²⁰ However, to our knowledge, no predictor of LVEF deterioration in patients with HFmrEF has been identified. In our cohort, 18% of the patients with HFmrEF died within 2 years of a cardiac cause. Of note, among HFmrEF patients, only those with vwUV of <7.50 showed subsequent LVEF deterioration, typically within 1 year after ablation, followed by HFO in the majority. These data suggest that the reduction of vwUV may precede LVEF deterioration. A critical reduction in vwUV may identify patients at risk, thus supporting an approach of early screening

for advanced HF management such as LVAD placement and HT.

STUDY LIMITATIONS. This was a single-center, observational, and retrospective study. The relatively small sample size and the low number of events are limitations. Considering the low number of events, the goodness-of-fit test was used to support our hypothesis. The results, including the cutoff values, need to be validated in a larger prospective cohort.

Integrated BV and UV were corrected for LV surface area obtained from EAM and AWT measured by echocardiography. This was based on the assumption that DCM or HNDCM patients have more uniform LV wall thinning. Of note, a strong correlation was noted between AWT measured by echocardiography and CT.

The antiarrhythmic and HF management after ablation was left to the discretion of the referring cardiologist, which may have influenced the outcome in some patients.

CONCLUSIONS

VwUV is a newly proposed surrogate for the amount of LV viable myocardium and is available from routine endocardial mapping. Because of its excellent accuracy for identifying patients at high risk for rapid progression to end-stage HF, vwUV may serve as an important prognostic tool in patients with DCM and VAs.

FUNDING SUPPORT AND AUTHOR DISCLOSURES

The Department of Cardiology Leiden receives unrestricted research and fellowship grants from Edward Lifesciences, Boston Scientific, Medtronic, and Biotronik. All authors have reported that they have no relationships relevant to the contents of this paper to disclose.

ADDRESS FOR CORRESPONDENCE: Dr Katja Zeppenfeld, Department of Cardiology (C-05-P), Leiden University Medical Center, P.O. Box 9600, 2300 RC Leiden, the Netherlands. E-mail: k.zeppenfeld@lumc.nl.

PERSPECTIVES

COMPETENCY IN MEDICAL KNOWLEDGE:

VwUV is available from routine voltage mapping, and its significant reduction was a strong predictor and the only independent predictor of HFO in patients with DCM and VT. Furthermore, vwUV predicted subsequent LVEF deterioration and HFO in patients with DCM with mildly reduced LVEF at the time of mapping.

TRANSLATIONAL OUTLOOK: The results suggest that a critical reduction of vwUV, as a surrogate for the total remaining viable myocardium at the time of evaluation, provides incremental prognostic information and may identify patients with DCM at risk for rapidly progressive HF. Further studies are needed to validate the outcome in a prospective manner.

REFERENCES

- Seferović PM, Polovina M, Bauersachs J, et al. Heart failure in cardiomyopathies: a position paper from the Heart Failure Association of the European Society of Cardiology. *Eur J Heart Fail*. 2019;21:553-576.
- aus dem Siepen F, Buss SJ, Messroghli D, et al. T1 mapping in dilated cardiomyopathy with cardiac magnetic resonance: quantification of diffuse myocardial fibrosis and comparison with endomyocardial biopsy. *Eur Heart J Cardiovasc Imaging*. 2015;16:210-216.
- Nakamori S, Dohi K, Ishida M, et al. Native T1 mapping and extracellular volume mapping for the assessment of diffuse myocardial fibrosis in dilated cardiomyopathy. *J Am Coll Cardiol Img*. 2018;11:48-59.
- Puntmann VO, Carr-White G, Jabbour A, et al. T1-mapping and outcome in nonischemic cardiomyopathy: all-cause mortality and heart failure. *J Am Coll Cardiol Img*. 2016;9:40-50.
- Vita T, Grani C, Abbasi SA, et al. Comparing CMR mapping methods and myocardial patterns toward heart failure outcomes in nonischemic dilated cardiomyopathy. *J Am Coll Cardiol Img*. 2019;12:1659-1669.
- Glashan CA, Androulakis AFA, Tao Q, et al. Whole human heart histology to validate electro-anatomical voltage mapping in patients with non-ischaemic cardiomyopathy and ventricular tachycardia. *Eur Heart J*. 2018;39:2867-2875.
- Hutchinson MD, Gerstenfeld EP, Desjardins B, et al. Endocardial unipolar voltage mapping to detect epicardial ventricular tachycardia substrate in patients with nonischemic left ventricular cardiomyopathy. *Circ Arrhythm Electrophysiol*. 2011;4:49-55.
- Muser D, Nucifora G, Castro SA, et al. Myocardial substrate characterization by CMR T1 mapping in patients with NICM and no LGE undergoing catheter ablation of VT. *J Am Coll Cardiol EP*. 2021;7:831-840.
- Pinto YM, Elliott PM, Arbustini E, et al. Proposal for a revised definition of dilated cardiomyopathy, hypokinetic non-dilated cardiomyopathy, and its implications for clinical practice: a position statement of the ESC Working Group on Myocardial and Pericardial Diseases. *Eur Heart J*. 2016;37:1850-1858.
- Lang RM, Badano LP, Mor-Avi V, et al. Recommendations for cardiac chamber quantification by echocardiography in adults: an update from the American Society of Echocardiography and the European Association of Cardiovascular Imaging. *J Am Soc Echocardiogr*. 2015;28:1-39.e14.
- McDonagh TA, Metra M, Adamo M, et al. 2021 ESC guidelines for the diagnosis and treatment of acute and chronic heart failure. *Eur Heart J*. 2021;42:3599-3726.
- Ebert M, Wijnmaalen AP, de Riva M, et al. Prevalence and prognostic impact of pathogenic variants in patients with dilated cardiomyopathy referred for ventricular tachycardia ablation. *J Am Coll Cardiol EP*. 2020;6:1103-1114.
- Campos B, Jauregui ME, Park KM, et al. New unipolar electrogram criteria to identify irreversibility of nonischemic left ventricular cardiomyopathy. *J Am Coll Cardiol*. 2012;60:2194-2204.
- Frankel DS, Liang JJ, Supple G, et al. Electrophysiological predictors of transplantation and

left ventricular assist device-free survival in patients with nonischemic cardiomyopathy undergoing ventricular tachycardia ablation. *J Am Coll Cardiol EP*. 2015;1:398-407.

15. Muser D, Santangeli P, Castro SA, et al. Long-Term Outcome After Catheter Ablation of Ventricular Tachycardia in Patients With Nonischemic Dilated Cardiomyopathy. *Circ Arrhythm Electrophysiol*. 2016;9:e004328.

16. Dinov B, Schratte A, Schirripa V, et al. Procedural outcomes and survival after catheter ablation of ventricular tachycardia in relation to electroanatomical substrate in patients with nonischemic-dilated cardiomyopathy: the role of unipolar voltage mapping. *J Cardiovasc Electro-physiol*. 2015;26:985-993.

17. Sasaki T, Miller CF, Hansford R, et al. Impact of nonischemic scar features on local ventricular electrograms and scar-related ventricular tachycardia circuits in patients with nonischemic cardiomyopathy. *Circ Arrhythm Electrophysiol*. 2013;6:1139-1147.

18. Desjardins B, Yokokawa M, Good E, et al. Characteristics of intramural scar in patients with nonischemic cardiomyopathy and relation to intramural ventricular arrhythmias. *Circ Arrhythm Electrophysiol*. 2013;6:891-897.

19. Piers SR, Tao Q, van Huls van Taxis CF, et al. Contrast-enhanced MRI-derived scar patterns and associated ventricular tachycardias in nonischemic cardiomyopathy: implications for the ablation

strategy. *Circ Arrhythm Electrophysiol*. 2013;6:875-883.

20. Savarese G, Vedin O, D'Amario D, et al. Prevalence and prognostic implications of longitudinal ejection fraction change in heart failure. *J Am Coll Cardiol HF*. 2019;7:306-317.

KEY WORDS dilated cardiomyopathy, electroanatomical mapping, heart failure, unipolar voltage, ventricular tachycardia

APPENDIX For a supplemental methods section, figures, and tables, please see the online version of this paper.